Int. J. Heat Mass Transfer Vol. 11, pp. 1027–1040. Pergamon Press 1968. Printed in Great Britain

CONVECTIVE HEAT TRANSFER IN ROTATING RADIAL CIRCULAR PIPES

(1ST REPORT, LAMINAR REGION)

YASUO MORI and WATARU NAKAYAMA

Department of Mechanical Engineering, Tokyo Institute of Technology, Tokyo, Japan

(*Received* 15 *October* 1967)

Abstract—A fully developed laminar flow field and temperature field in a pipe rapidly rotating around a perpendicular axis are analyzed theoretically, by assuming velocity and temperature boundary layers along the pipe wall. The resistance coefficient and the Nusselt number are obtained in the region of large values of (N/χ). The parameter N is the product of Re and $\hat{\omega}$, where $\hat{\omega}$ is the ratio of Coriolis force to viscous force, and χ represents the effect of Coriolis force caused by the secondary flow. It is shown that the resistance coefficient and the Nusselt number increase remarkably, due to a secondary flow driven by Coriolis force. It is also shown by analyzing the two wall temperature conditions, i.e. the constant wall temperature gradient and the uniform wall temperature, that the Nusselt number is almost the same for both these conditions.

NOMENCLATURE

A, w_1 at the center of a cross section perpendicular to the pipe axis;
A', g_1 at the center of a cross section perpendicular to the pipe axis;
a, radius of the pipe;
C, $= -(\partial P'/\partial z)$;
c_p, specific heat of fluid at constant pressure;
D, intensity of the secondary flow in the flow core [dimensionless];
$f_{zr}, f_{z\psi}$, tangential stresses in the z direction of fluid;
G, $= T_w - T$;
g, dimensionless temperature, $= G/\tau a$;
k, heat conductivity of fluid;
N, $= \hat{\omega}\, Re$;
$\bar{N}$, normalized constant;
Nu, Nusselt number, $= 2aQ_{wm}/k(T_w - T_m)$;
Nu_o, Nusselt number for the Poiseuille flow (48/11 for constant heat flux case, 3·66 for isothermal case);
P, dimensionless pressure, $= (a^2/\nu^2)(p/\rho)$;
P', $= P - (\frac{1}{8})\hat{\omega}^2 z^2$;
Pr, Prandtl number;
p, pressure;
Q_w, heat flux at the wall to the fluid;
q_r, q_ψ, heat flux in the fluid;
Re, Reynolds number, $= 2aW_m/\nu$;
r, co-ordinate in radial direction in a cross section perpendicular to the pipe axis;
T, temperature;
T_m, mixed mean fluid temperature;
T_w, wall temperature;
U, radial component of velocity, $u = Ua/\nu$ [dimensionless];
V, circumferential component of velocity, $v = Va/\nu$ [dimensionless];
W, axial component of velocity, $w = Wa/\nu$ [dimensionless];
W_m, mean velocity, $w_m = W_m a/\nu$ [dimensionless];
$\bar{X}$, equation (72);
Z, co-ordinate along the pipe axis, $z = Z/a$ [dimensionless].

Greek symbols

α'_0, the minimum eigenvalue, $\alpha_0 = a\alpha'_0$;
δ, dimensionless thickness of velocity boundary layer;

δ_T, dimensionless thickness of thermal boundary layer;
ζ, $=\delta_T/\delta$;
H, $=R/a$;
η, $=r/a$;
λ, resistance coefficient,

$$= \left(-\frac{\partial p}{\partial Z}\right)\frac{2a}{\frac{1}{2}\rho W_m^2};$$

λ_0, resistance coefficient for the Poiseuille flow, $=64/Re$;
λ^*, $=\lambda + (4\hat{\omega}^2/Re^2)(Z/a)$;
μ, viscosity;
ν, $=\mu/\rho$;
ξ, $=1-\eta$;
ρ, density;
$\tau_{z\eta}$, $=(a^2/\nu^2)(f_{z\eta}/\rho)$;
$\tau_{z\psi}$, $=(a^2/\nu^2)(f_{z\psi}/\rho)$;
τ, temperature gradient along the pipe axis (constant);
ψ, circumferential co-ordinate in a cross section perpendicular to the pipe axis;
χ, parameter, $=\sqrt{[1 + 1{\cdot}25\,(\hat{\omega}/Re)^2]} - 1{\cdot}118\,(\hat{\omega}/Re)$;
ω, angular velocity of the pipe;
$\hat{\omega}$, $=2a^2\omega/\nu$.

Subscripts

0, value at the pipe wall;
1, value in the flow core region;
m, mean value taken around the periphery ($\psi = -\pi \sim \pi$);
δ, value at $\xi = \delta$;
δ_T, value at $\xi = \delta_T$.

1. INTRODUCTION

THE INCREASE in the turbine inlet temperature of gas turbine engines is an urgent need today to obtain a higher efficiency in the engines of aircraft, ships and many other industrial facilities. Parallel with the evolution of metals working in high temperature, several methods of cooling rotor blades have been tried and developed. Cooled blades are widely used in modern engines. Commonly used methods are those of radial pass cooling and thermo syphone. The former is achieved by flowing a cooling fluid through narrow radial passes in a blade, while in the latter, holes with closed ends at the tip of each blade are filled with coolants. Fundamental understanding and design data of these methods are still short, and there is a need for more knowledge about heat-transfer mechanisms in these narrow passages.

The purpose of the present study is to investigate, theoretically and experimentally, heat transfer in a straight circular pipe rotating around the vertical axis. In this paper, a theoretical analysis in a laminar region is reported. It is thought that Coriolis force causes a secondary flow in a rotating pipe, and the secondary flow makes the heat-transfer rate higher than that in a stationary pipe. As a matter of course, practical interest is in the area of flow rate and rotating speed where the secondary flow is intense and makes a remarkable effect on the heat-transfer rate.

When a body force working on a fluid is in the direction vertical to the pipe axis, a secondary flow is produced. The authors have reported the studies of cases when an effective secondary flow is caused by centrifugal force and buoyancy [1–4]. Under the strong effect from secondary flows, the velocity and temperature distributions in a pipe have a characteristic profile showing that their gradient of change is moderate in most of the regions of a cross section of the pipe and a steep gradient is found only in a thin layer adjacent to the pipe wall. It is shown that the effect of secondary flow predominates over almost the whole of a cross section except in the neighborhood of the pipe wall, and the influence of viscosity and heat conduction is confined mainly to the same very thin layer next to the wall. In order to analyse heat transfer in this kind of flow, flow and temperature fields may be divided into two regions, a core region occupying a greater part of the pipe and a boundary layer next to the wall.

In the present paper, the flow is assumed to be steady and fully developed, and analysis done by the flow code and boundary-layer concept.

The analytical procedure is the same as that used by the authors for a curved pipe and for a straight pipe rotating around a parallel axis [1, 4].

2. THE ANALYSIS OF THE FLOW IN A ROTATING PIPE

2.1. *The fundamental equations*

The system of co-ordinates is taken as shown in Fig. 1. The symbol a is a radius of the pipe, ω is angular velocity and Z is the co-ordinate taken along the pipe axis from the axis of rotation toward the outer side and $Z \geqslant r$ is assumed.

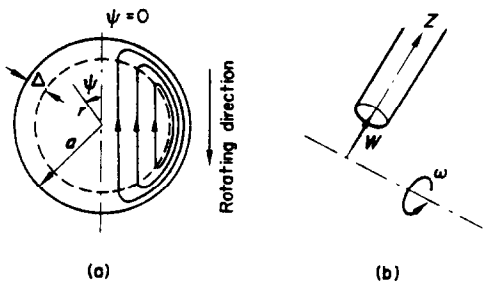

FIG. 1. System of co-ordinates.

Since a secondary flow is set up as shown in Fig. 1, we take circumferential co-ordinate ψ from the stream line of the secondary flow passing through the center of a cross section.

The velocity components of r-, ψ- and Z-direction are denoted respectively U, V, W the pressure p, density ρ and the kinematic viscosity ν. The following non-dimensional quantities are defined:

$$\eta = r/a, \quad u = Ua/\nu, \quad v = Va/\nu$$

$$w = Wa/\nu, \quad z = Z/a, \quad P = (a^2/\nu^2)(p/\rho).$$

We denote the tangential stress on a small volume of the fluid as shown in Fig. 2 as $f_{z\eta}$, $f_{z\psi}$ and the non-dimensional quantities as $\tau_{z\eta} = (a^2/\nu^2)(f_{z\eta}/\rho)$, $\tau_{z\psi} = (a^2/\nu^2)(f_{z\psi}/\rho)$. Then the force balance equation in the direction of the pipe axis is expressed as follows;

$$\frac{\partial}{\eta\,\partial\eta}(\eta\tau_{z\eta}) + \frac{\partial\tau_{z\psi}}{\eta\,\partial\psi} = \frac{\partial P}{\partial z} - \frac{\hat{\omega}^2}{4}z + \hat{\omega}(u\cos\psi - v\sin\psi) \qquad (1)$$

where $\hat{\omega} = 2a^2\omega/\nu$. The second term in the right-hand side of equation (1) represents the centrifugal force; the third term the Coriolis force in the direction of the pipe axis.

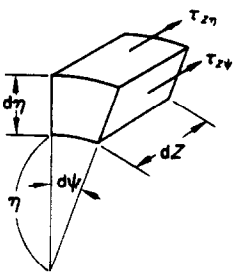

FIG. 2. Shear stresses exerting on a small element of fluid.

These terms are characteristic to the present problem and do not appear in the equations for a curved pipe [1, 2], a horizontal pipe [3], or a circular pipe rotating around a parallel axis [4].

The tangential stress may be expressed as follows:

$$\left.\begin{aligned}\tau_{z\eta} &= \frac{\partial w}{\partial\eta} - uw \\ \tau_{z\psi} &= \frac{\partial w}{\eta\,\partial\psi} - vw.\end{aligned}\right\} \qquad (2)$$

Now the pressure term is divided into that due to centrifugal force and that due to secondary flow, and written so that

$$P = \tfrac{1}{8}\hat{\omega}^2 z^2 + P'. \qquad (3)$$

For a fully developed flow, the z-direction gradient of P' is constant. Hence we have:

$$-(\partial P'/\partial z) = C\,(\text{constant}). \qquad (4)$$

2.2. *Velocity in the flow core*

Most of the pipe is occupied by the flow core.

We give a subscript 1 to the symbols in the flow core region where stresses caused by the secondary flow predominate.

We put $\tau_{z\eta} = -u_1 w_1$, $\tau_{z\psi} = -v_1 w_1$, in equation (2) and substitute these into equations (1–4)

$$u_1 \frac{\partial w_1}{\partial \eta} + \frac{v_1}{\eta} \frac{\partial w_1}{\partial \psi} + \hat{\omega}(u_1 \cos\psi - v_1 \sin\psi) = C. \tag{5}$$

Since the pressure gradient and the Coriolis force in a cross section are assumed to be in balance with each other in the flow core,

$$\left.\begin{aligned} \frac{\partial P_1}{\partial \eta} &= \hat{\omega} w_1 \cos\psi \\ \frac{\partial P_1}{\eta \partial \psi} &= -\hat{\omega} w_1 \sin\psi. \end{aligned}\right\} \tag{6}$$

Therefore, the secondary flow is approximated by a uniform flow as shown in Fig. 1. So as to satisfy the equation of continuity, $\partial(\eta u_1)/\eta\,\partial\eta + \partial v_1/\eta\,\partial\psi = 0$. We put radial velocity component u and circumferential component v as follows, using constant D,

$$u_1 = D\cos\psi, \qquad v_1 = -D\sin\psi. \tag{7}$$

From equation (6), the following condition is obtained,

$$\frac{\partial w_1}{\eta\,\partial\psi}\cos\psi + \frac{\partial w_1}{\partial\eta}\sin\psi = 0. \tag{8}$$

As a particular solution to satisfy equations (5) and (8), w_1 is expressed as follows;

$$w_1 = A + \left(\frac{C}{D} - \hat{\omega}\right)\eta\cos\psi \tag{9}$$

where A is constant. Equation (9) is different from the expression of w_1 for a curved pipe [1, 2] only by the term $\hat{\omega}\eta\cos\psi$ representing the effect of Coriolis force in the direction of the pipe axis.

The axial velocity w_1 of equation (9) represents a distribution described by a solid line in Fig. 3.

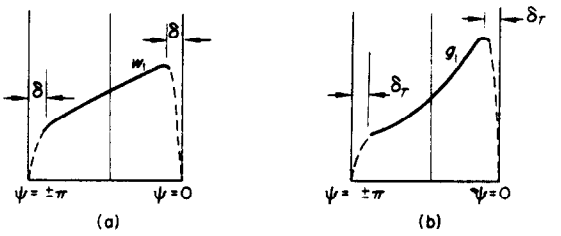

FIG. 3. w and g.

2.3. *The velocity distribution in the boundary layer*

The boundary-layer approximation can be applied to a thin layer next to the wall. In this sense, the layer is called a boundary layer. The dimensionless thickness of the boundary layer, the thickness divided by the pipe radius a, is denoted by $\delta(\ll 1)$ and the distance from the pipe wall is denoted by $\xi(= 1 - \eta)$.

So as to satisfy the boundary conditions;

$$\text{at} \quad \xi = \delta \qquad w = w_{1\delta}, \qquad \frac{\partial w}{\partial \xi} = -\frac{\partial w_1}{\partial \eta}$$

as shown by the dotted lines in Fig. 3, we put w in the boundary layer as follows:

$$w = w_{1\delta}\left(2\frac{\xi}{\delta} - \frac{\xi^2}{\delta^2}\right) + \delta\left(\frac{C}{D} - \hat{\omega}\right) \times \cos\psi\left(\frac{\xi}{\delta} - \frac{\xi^2}{\delta^2}\right) \tag{10}$$

where the suffix δ represents the value at the edge of the boundary layer.

So as to satisfy $v = v_1$, $\partial v/\partial\xi = 0$ at $\xi = \delta$ and also the condition of the flux continuity of the secondary flow in the flow core and in the boundary layer (1) we put the circumferential velocity component v as follows,

$$v = -D\sin\psi\left[\left(-\frac{12}{\delta} + 6\right)\frac{\xi}{\delta} + \left(\frac{24}{\delta} - 9\right) \times \frac{\xi^2}{\delta^2} + \left(-\frac{12}{\delta} + 4\right)\frac{\xi^3}{\delta^3}\right]. \tag{11}$$

Since we are considering a fully developed flow, the thickness of the boundary layer δ is constant

in the direction of the pipe axis (z) but varies with ψ.

However, since the variation is assumed to be very small [1], δ is regarded as the mean value between $\psi = -\pi$ and $\psi = \pi$ and it is treated as a constant hereafter.

2.4. *The relation between A, C, D and δ*

When the Reynolds number is given, it is necessary to know the quantities A, D, C and δ in the equations of velocity distributions (7, 9, 10, 11). There are two equations relating A and C to δ as shown below. One of them is the expression of the mean velocity of fluid in the pipe W_m. When the Reynolds number is defined as $Re = 2aW_m/\nu$, the non-dimensional mean velocity w_m is expressed as follows;

$$w_m = \frac{Re}{2} = \frac{1}{\pi}\left\{\int_{-\pi}^{\pi}\int_{0}^{1-\delta} w_1 \eta \, d\eta \, d\psi + \int_{-\pi}^{\pi}\int_{0}^{\delta} w(1-\xi)\, d\xi \, d\psi\right\}. \quad (12)$$

Substituting equations (9) and (10) into equation (10), A is given as follows;

$$A = \frac{Re}{2}\frac{1}{1 - \frac{2}{3}\delta + \frac{1}{6}\delta^2}. \quad (13)$$

The other relation is obtained by integrating equation (1) over a cross section. The equation expressing the force balance of a fluid element bounded by the pipe wall is given as follows:

$$\int_{-\pi}^{\pi}\left(\frac{\partial w}{\partial \xi}\right)_0 d\psi \qquad \int_{-\pi}^{\pi}\int_{0}^{1}\left(-\frac{\partial P'}{\partial z}\right)\eta \, d\eta \, d\psi \quad (14)$$

where the subscript 0 denotes the value at the pipe wall.

Using equation (4) and giving the suffix m to the mean value between $\psi = -\pi$ and $\psi = \pi$, we rewrite equation (14) in a non-dimensional form

$$\left(\frac{\partial w}{\partial \xi}\right)_{0m} = \frac{C}{2}. \quad (15)$$

Substituting equation (10) into equation (15),

$$C = \frac{4A}{\delta} = \frac{2Re}{\delta}\frac{1}{1 - \frac{2}{3}\delta + \frac{1}{6}\delta^2}. \quad (16)$$

By equations (13) and (16), the unknown quantities are reduced to two, D and δ.

In order to calculate these quantities, we use the following momentum integral equations for the boundary layer.

2.5. *The momentum integral equations of the boundary layer*

By substituting equation (2) into equation (1) and making a boundary-layer approximation, the following momentum integral equation of the boundary layer in z-direction is obtained.

$$\left(\frac{\partial w}{\partial \xi}\right)_0 = w_{1\delta}\frac{\partial}{\partial \psi}\int_0^{\delta} v \, d\xi - \frac{\partial}{\partial \psi}\int_0^{\delta} vw \, d\xi + \hat{\omega}\sin\psi \int_0^{\delta} v \, d\xi + C\delta. \quad (17)$$

The third term in the right-hand side of equation (17) comes from Coriolis force due to secondary flow. This term does not appear in the analysis for a curved pipe [1] or a pipe rotating around the parallel axis [4]. The Coriolis force, due to the velocity component in the direction of pipe axis, is perpendicular to the main flow, while the Coriolis force due to the secondary flow and angular velocity is in the direction of the pipe axis. This secondary Coriolis force gives a characteristic influence on the flow dealt with in the present problem, particularly in the case of a large angular velocity.

Substitution of equations (9–11) into the right-hand side of equation (7) yields the following expression of

$$\left(\frac{\partial w}{\partial \xi}\right)_0 = E + F\cos\psi \quad (18)$$

$$E = \left[\left(\tfrac{2}{5} - \tfrac{2}{15}\delta\right)\cos^2\psi + \left(\tfrac{3}{5} - \tfrac{28}{15}\delta\right)\sin^2\psi\right] \times (C - \hat{\omega}D) + \hat{\omega}D(1-\delta)\sin^2\psi + C\delta \quad (19)$$

$$F = AD\left(\tfrac{2}{5} - \tfrac{7}{15}\delta\right). \quad (20)$$

The mean value of $(\delta w/\delta\xi)_0$ between $\psi = -\pi$ and $\psi = \pi$ given by equation (18) is equal to $C/2$, if $\hat{\omega}/Re < 1/\delta$ is assumed. This mean value coincides with that given by equation (15) which is obtained by considering the total force balance upon the fluid.

The variation of E with ψ seems to be small compared with $F\cos\psi$ as shown in [1].

Thus, we replace E in equation (18) by its mean value $C/2$. On the other hand, $(\partial w/\partial\xi)_0$ from equation (10) is written as

$$\left(\frac{\partial w}{\partial \xi}\right)_0 = \frac{C}{2} + \frac{1}{\delta}\left(\frac{C}{D} - \hat{\omega}\right)(2 - \delta)\cos\psi. \quad (21)$$

Then we let the coefficient of $\cos\psi$ in equation (18), that is F, be equal to that of $\cos\psi$ in equation (21).

Neglecting the terms with the order of magnitude smaller than $\delta^2(\ll 1)$, we have the following equation:

$$D^2\delta^2 + 10\frac{\hat{\omega}}{Re}D\delta = 20(1 + \tfrac{2}{3}\delta). \quad (22)$$

The second term in the left-hand side of equation (22) represents the effect of the Coriolis force due to secondary flow, and it has not been found in the previous analysis [1–4].

The momentum integral equation in the circumferential (ψ) direction is expressed as follows;

$$\left(\frac{\partial v}{\partial \xi}\right)_0 = -\int_0^\delta \frac{\partial P}{\partial \psi}\,d\xi - \hat{\omega}\sin\psi\int_0^\delta w\,d\xi + v_1\frac{\partial}{\partial\psi}\int_0^\delta v\,d\xi - \frac{\partial}{\partial\psi}\int_0^\delta v^2\,d\xi. \quad (23)$$

In order to obtain the equation which is necessary for the determination of the mean value of the boundary-layer thickness δ, both sides of equation (23) are averaged between $\psi = 0$ and π. The equation expresses the relationship between the pressure gradient, body (Coriolis) force in the boundary layer and the frictional resistance against the secondary flow at the wall as follows:

$$\left(\frac{\partial v}{\partial \xi}\right)_{0m} = -\int_0^\delta \left[\frac{\partial P}{\partial \psi}\right]_m d\xi - \hat{\omega}\left[\sin\psi\int_0^\delta w\,d\xi\right]_m. \quad (24)$$

From the momentum balance in a radial direction, the pressure gradient is written so that

$$\frac{\partial P}{\partial \psi} = \left(\frac{\partial P_1}{\partial \psi}\right)_\delta + \frac{\partial}{\partial\psi}\int_\xi^\delta (v^2 + \hat{\omega}w\cos\psi)\,d\xi. \quad (25)$$

The first term in the right-hand side of equation (25) is written in terms of the Coriolis force at $\xi = \delta$ from equation (6). Thus, the first term in the right-hand side of equation (24) becomes

$$\left[\int_0^\delta \frac{\partial P}{\partial \psi}\,d\xi\right]_m = (-\hat{\omega}A\delta - \tfrac{7}{12}\hat{\omega}A\delta^2)[\sin\psi]_m. \quad (26)$$

From equation (11),

$$\left(\frac{\partial v}{\partial \xi}\right)_{0m} = \frac{12D}{\delta^2}\left(1 - \frac{\delta}{2}\right)[\sin\psi]_m. \quad (27)$$

After substituting equations (26) and (27) into equation (24), we have the following equation:

$$\frac{12D}{\delta^2}\left(1 - \frac{\delta}{2}\right) = \tfrac{1}{3}A\hat{\omega}\delta(1 + \tfrac{7}{4}\delta). \quad (28)$$

Equation (28) is rewritten as follows by substituting A from equation (13);

$$\frac{D}{\delta^2} = \frac{\delta}{72}Re\,\hat{\omega}(1 + \tfrac{35}{12}\delta). \quad (29)$$

In order to obtain D and δ from equations (22) and (29), we expand them in series as follows:

$$\begin{aligned} D &= D_1 + D_2 \qquad D_1 \gg D_2 \\ \delta &= \delta_1 + \delta_2 \qquad \delta_1 \gg \delta_2. \end{aligned} \quad (30)$$

Substitution of equation (30) into equations (22)

and (28) and use of parameters.

$$N = \hat{\omega}\, Re$$

$$\chi = \sqrt{\left[1 + 1{\cdot}25\left(\frac{\hat{\omega}}{Re}\right)^2\right]} - 1{\cdot}118\left(\frac{\hat{\omega}}{Re}\right)$$

yield the following results of first order approximation.

$$D_1 = 1{\cdot}056\, N^{\frac{1}{2}}\chi^{\frac{1}{2}} \tag{31}$$

$$\delta_1 = 4{\cdot}236\, N^{-\frac{1}{2}}\chi^{\frac{1}{2}}. \tag{32}$$

When we substitute equations (31) and (32) into equations (22) and (29) and pick out the second order approximation terms from equation (22),

$$8{\cdot}472\, D_2 + 2{\cdot}112\, N^{\frac{1}{2}}\chi^{\frac{1}{2}}\delta_2 = \frac{56{\cdot}48}{(\sqrt{20})\,\chi + \dfrac{5\hat{\omega}}{Re}}. \tag{33}$$

From equation (29)

$$D_2 - 0{\cdot}748\, N^{\frac{1}{2}}\chi^{\frac{1}{2}}\delta_2 = 0{\cdot}373\,\chi. \tag{34}$$

From equations (33) and (34), is found that

$$\left.\begin{aligned}\delta_2 &= \frac{6{\cdot}685}{N^{\frac{1}{2}}\chi^{\frac{1}{2}}\left(4{\cdot}473\,\chi + \dfrac{5\hat{\omega}}{Re}\right)} \times \left[1 - 2{\cdot}848\,\chi\left(\frac{\hat{\omega}}{Re}\right) - 2{\cdot}547\,\chi^2\right] \\ D_2 &= \frac{4{\cdot}999}{4{\cdot}473\,\chi + \dfrac{5\hat{\omega}}{Re}} \times \left[1 - 0{\cdot}983\,\chi\left(\frac{\hat{\omega}}{Re}\right) - 0{\cdot}879\right].\end{aligned}\right\} \tag{35}$$

2.6. *The resistance coefficient*

The resistance coefficient λ is defined below, and this is written by use of equations (3) and (4) in terms of non-dimensional quantities.

$$\left(-\frac{\partial p}{\partial Z}\right)\frac{2a}{\frac{1}{2}\rho W_m^2} = -\frac{4\hat{\omega}^2}{Re^2}\left(\frac{Z}{a}\right) + \frac{16C}{Re^2}.$$

The resistance coefficient is obtained by putting $C = (2Re/\delta)\,[1 - \frac{2}{3}\delta]$ from equation (16) in the above equation. When N/χ is larger than 10^5, it is found that the magnitude of δ_2 calculated by equation (35) gives a correction only less than a few per cent on δ. Therefore, we use δ_1, given by equation (32) as δ. The ratio of λ^* to the resistance coefficient for Poiseuille flow, $\lambda_0 = 64/Re$, is given by

$$\frac{\lambda^*}{\lambda_0} = 0{\cdot}118\left(\frac{N}{\chi}\right)^{\frac{1}{4}}\frac{1}{1 - 2{\cdot}82\left(\dfrac{N}{\chi}\right)^{-\frac{1}{4}}}. \tag{36}$$

The curve of λ^*/λ_0 is shown in Fig. 4. In Fig. 4, the asymptotic straight line for the case $\delta \to 0$ is also shown. As shown in the analysis for curved pipe [1], the curve to be obtained by higher approximation would come in between the asymptotic straight line and the curved line given by equation (36), rather close to the curved line.

The experimental values obtained by Trefethen [5], using water, are shown in Fig. 4.

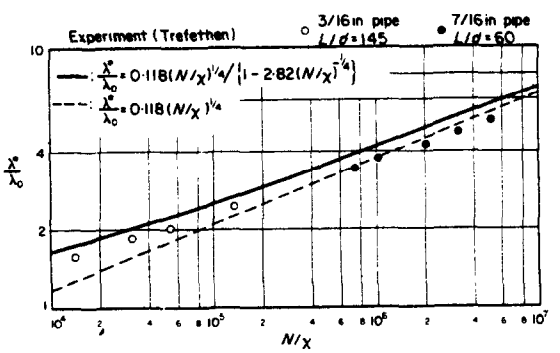

FIG. 4. λ^*/λ_0 vs. (N/χ).

The open circles are for the case of L/d (L: the pipe length between the pressure measuring taps, d: the diameter of pipe) = 145, and the solid circles are for $L/d = 60$. The open circles which are obtained by use of a sufficiently large L/d agree considerably well with the theoretical result. The solid circles are for the flow which is

not thought to be fully developed because of the small L/d. It is of course necessary to determine the availability of the present theoretical result by a more sufficient amount of experiments.

3. THE ANALYSIS IN THE TEMPERATURE FIELD

3.1. *The analysis under the condition of a constant wall temperature gradient*

3.1.1. *The fundamental equation.* In a fully developed temperature field, the temperature gradient in the axial (Z) direction has the same value all over the region; therefore, temperature T is expressed in the form

$$T = \tau Z - G(r, \psi) \tag{37}$$

where τ is a constant temperature gradient in the axial (Z) direction and $G(r, \psi)$ is the function of r and ψ.

The wall temperature T_w is assumed to be invariable around the periphery of a cross section. Hence,

$$T_w = \tau Z.$$

The boundary condition for G is: $G = 0$ at $r = a$.

Dimensionless temperature is defined as $g = G/\tau a$. The energy equation is written in dimensionless form as

$$\frac{\partial}{\eta \partial \eta}(\eta q_\eta) + \frac{\partial q_\psi}{\eta \partial \psi} = w \tag{38}$$

where q_η, q_ψ are dimensionless heat fluxes in the fluid in the radial (η) and circumferential (ψ) directions respectively.

These heat fluxes are expressed as

$$\left.\begin{aligned} q_\eta &= -\frac{1}{Pr}\frac{\partial g}{\partial \eta} + ug \\ q_\psi &= -\frac{1}{Pr}\frac{\partial g}{\eta \partial \psi} + vg. \end{aligned}\right\} \tag{39}$$

3.1.2. *The temperature distribution in the flow core.* In the core region, the heat flux transferred by the secondary flow is considered to be predominant.

Thus we have, from equation (36),

$$q_\eta = u_1 g_1, \qquad q_\psi = v_1 g_1. \tag{40}$$

Substitution of equation (40) into equation (38) yields the following energy equation;

$$u_1 \frac{\partial g_1}{\partial \eta} + v_1 \frac{\partial g_1}{\eta \partial \psi} = w_1. \tag{41}$$

After substituting equations (7) and (9) into equation (41), we put g_1, the particular solution for equation (41), as

$$g_1 = A' + \frac{1}{2D}\left(\frac{C}{D} - \hat{\omega}\right)\eta^2 + \frac{A}{D}\eta \cos\psi \tag{42}$$

where A' is constant.

As shown in Fig. 3(b), the distribution of g_1 has a profile similar to that observed in a curved pipe under a remarkable effect of the secondary flow.

The expression of g_1 by equation (42) differs from that obtained in the analysis for a curved pipe [1] only in the coefficient of η^2 where $\hat{\omega}$ is introduced by Coriolis force due to a secondary flow.

3.1.3. *Temperature in the boundary layer.* The temperature distribution in the boundary layer is determined so as to meet g_1 at the edge of the boundary layer as shown by dotted lines in Fig. 3(b).

In order to consider the influence of Prandtl numbers, a thermal boundary layer of dimensionless thickness δ_T is assumed along the pipe wall. The ratio of δ_T to δ is denoted by $\zeta(= \delta_T/\delta)$.

We put g in the same form with that used in the analysis for a curved pipe [1].

$$g = g_{1\delta}\left[\frac{2}{\zeta}\left(\frac{\xi}{\delta} - 2\frac{\xi^2}{\delta^2} + \frac{\xi^3}{\delta^3}\right) + 3\frac{\xi^2}{\delta^2} - 2\frac{\xi^3}{\delta^3}\right] + \delta\left[\frac{C}{D^2}(1 - \delta) + \frac{A}{D}\cos\psi\right]\left(\frac{\xi^2}{\delta^2} - \frac{\xi^3}{\delta^3}\right) \tag{43}$$

$$(\delta_T \leqslant \delta)$$

$$g = g_{1\delta_T}\left(2\frac{\xi}{\delta_T} - \frac{\xi^2}{\delta_T{}^2}\right) + \delta_T\left[\frac{C}{D^2}(1-\delta_T) + \frac{A}{D}\cos\psi\right] \times \left(\frac{\xi^2}{\delta_T^2} - \frac{\xi^3}{\delta_T^3}\right) \quad (44)$$

$$(\delta_T \geqslant \delta)$$

where $g_{1\delta}$ and $g_{1\delta_T}$ are g_1 at $\xi = \delta$ and δ_T respectively to be obtained from equation (42).

Since $\delta, \delta_T \ll 1$ we may put $g_{1\delta} \approx g_{1\delta_T}$.

3.1.4. *Determination of A'.* In order to obtain A', equation (38) is integrated over a whole cross section as follows:

$$\frac{1}{Pr}\int_{-\pi}^{\pi}\left(\frac{\partial g}{\partial \xi}\right)_0 \mathrm{d}\psi = \int_{-\pi}^{\pi}\int_0^1 w\eta\,\mathrm{d}\eta\,\mathrm{d}\psi = \frac{\pi}{2}Re. \quad (45)$$

Denoting the mean value around periphery ($\psi = -\pi \sim \pi$) by suffix m, we rewrite equation (45) in the following form:

$$\left(\frac{\partial g}{\partial \xi}\right)_{0m} = \frac{Re\,Pr}{4} \quad (46)$$

The gradient $(\partial g/\partial\xi)_0$ is calculated from equations (43) and (44) by neglecting the small terms for both cases of $\delta_T/\delta \gtrless 1$.

$$\left(\frac{\partial g}{\partial \xi}\right)_0 \approx \frac{2}{\zeta\delta}\left\{A' + \frac{Re}{D^2\delta}\left[1 - \frac{D\delta}{2}\left(\frac{\hat{\omega}}{Re}\right)\right]\right\} + \frac{Re}{\zeta D\delta}\cos\psi. \quad (47)$$

Substituting equation (47) into equation (46), we obtain A' as follows;

$$A' = \frac{\zeta\delta\,Re\,Pr}{8} - \frac{Re}{D^2\delta}\left[1 - \frac{D\delta}{2}\left(\frac{\hat{\omega}}{Re}\right)\right]. \quad (48)$$

3.1.5. *The energy integral equation of the boundary layer.* Heat fluxes due to convection and conduction are equally considered in the boundary layer. Use of the boundary-layer approximation and integration of the boundary-layer equation from $\xi = 0$ to δ yield the energy integral equation.

$$\frac{1}{Pr}\left(\frac{\partial g}{\partial \xi}\right)_0 = g_{1\delta}\frac{\partial}{\partial\psi}\int_0^\delta v\,\mathrm{d}\xi - \frac{\partial}{\partial\psi}\int_0^\delta gv\,\mathrm{d}\xi + \int_0^\delta w\,\mathrm{d}\xi. \quad (49)$$

From equation (49), $\zeta\ (=\delta_T/\delta)$ is obtained by a method similar to the one already shown in the analysis for a curved pipe [1]. The procedure is described below. We substitute equations (11) and (43) or equation (44) into equation (49) and make sure that the mean value of $(\partial g/\partial\xi)_0$ obtained from the energy integral equation of the boundary layer satisfies equation (46). Then, by putting $(\partial g/\partial\xi)_0$ of equation (49) equal to equation (47), the relation between ζ and the Prandtl numbers is obtained.

When $\delta_T \leqslant \delta$, from equation (49),

$$\left(\frac{\partial g}{\partial \xi}\right)_0 = E' + F'\cos\psi \quad (50)$$

where

$$E' = \frac{Re\,Pr}{2}\left[\left(\frac{22}{35} - \frac{8}{35\zeta}\right)\cos^2\psi + \left(\frac{8}{35\zeta} + \frac{13}{35}\right)\sin^2\psi\right] \quad (51)$$

$$F' = \frac{\zeta D\delta\,Re\,Pr^2}{8}\left(\frac{22}{35} - \frac{8}{35\zeta}\right). \quad (52)$$

The variation of E' with ψ is very small, so E' can be replaced by the mean value $Re\,Pr/4$.

From equations (47) and (50), ζ is obtained as

$$\zeta = \frac{2}{11}\left[1 + \sqrt{\left(1 + \frac{77}{4\chi}\frac{1}{Pr^2}\right)}\right]. \quad (53)$$

Equation (53) is applicable when $\delta_T \leqslant \delta$, that is,

$$\frac{\hat{\omega}}{Re} \leqslant \frac{Pr}{2{\cdot}236}\left(1 - \frac{1}{Pr^2}\right).$$

The result is also obtained when $\delta_T \geqslant \delta$.

$$\zeta = \frac{1}{5}\left[2 + \sqrt{\left(\frac{10}{\chi}\frac{1}{Pr^2} - 1\right)}\right]. \tag{54}$$

In this case, the applicable range is determined by

$$\frac{\hat{\omega}}{Re} \geqslant \frac{Pr}{2{\cdot}236}\left(1 - \frac{1}{Pr^2}\right).$$

3.1.6. *Nusselt number*. Nusselt number is defined by

$$Nu = \frac{2aQ_{wm}}{k(T_w - T_m)} \tag{55}$$

where Q_{wm} is the mean value of the heat flux at the wall around the periphery ($\psi = -\pi \sim \pi$).

Consideration of the heat balance over a whole cross section yields

$$Q_{wm} = \tfrac{1}{4}\tau k\, Re\, Pr. \tag{56}$$

The mixed mean fluid temperature T_m is defined by

$$T_m = \frac{1}{\pi a^2 W_m}\int_{-\pi}^{\pi}\int_{0}^{a} TWr\,\mathrm{d}r\,\mathrm{d}\psi. \tag{57}$$

The difference between T_m and wall temperature T_w is expressed as follows;

$$T_w - T_m = \begin{cases} \dfrac{2\tau a}{\pi Re}\left[\displaystyle\int_{-\pi}^{\pi}\int_{0}^{1-\delta} g_1 w_1 \eta\,\mathrm{d}\eta\,\mathrm{d}\psi + \int_{-\pi}^{\pi}\int_{0}^{\delta} gw\,\mathrm{d}\xi\,\mathrm{d}\psi\right] & (58) \\ \qquad\qquad (\text{for } \delta_T \leqslant \delta) & \\ \dfrac{2\tau a}{\pi Re}\left[\displaystyle\int_{-\pi}^{\pi}\int_{0}^{1-\zeta\delta} g_1 w_1 \eta\,\mathrm{d}\eta\,\mathrm{d}\psi + \int_{-\pi}^{\pi}\int_{\delta}^{\zeta\delta} gw_1\,\mathrm{d}\xi\,\mathrm{d}\psi + \int_{-\pi}^{\pi}\int_{0}^{\delta} gw\,\mathrm{d}\xi\,\mathrm{d}\psi\right] & (59) \\ \qquad\qquad (\text{for } \delta_T \geqslant \delta). & \end{cases}$$

The integrations in equations (58) and (59) are calculated by using equations (9, 10, 42, 43, 44). The Nusselt number Nu is obtained from equations (55, 56, 58) or (59). For the case that

$$\frac{\hat{\omega}}{Re} \leqslant \frac{Pr}{2{\cdot}236}\left(1 - \frac{1}{Pr^2}\right) \qquad (Pr \geqslant 1)$$

the ratio of Nu to the value of Nu for Poiseuille flow Nu_0 ($=48/11$) is expressed as

$$\frac{Nu}{Nu_0} = \frac{0{\cdot}216}{\zeta}\left(\frac{N}{\chi}\right)^{\frac{1}{3}} \Big/ \left\{1 - 4{\cdot}80\left[1 - \frac{0{\cdot}176}{\zeta} - \frac{0{\cdot}07}{\zeta\, Pr}\left(\frac{1}{\zeta} + 4{\cdot}33\right)\right]\left(\frac{N}{\chi}\right)^{-\frac{1}{3}}\right\}. \tag{60}$$

For the case that

$$\frac{\hat{\omega}}{Re} \geqslant \frac{Pr}{2{\cdot}236}\left(1 - \frac{1}{Pr^2}\right)$$

the ratio Nu/Nu_0 is obtained as

$$\frac{Nu}{Nu_0} = \frac{0{\cdot}216}{\zeta}\left(\frac{N}{\chi}\right)^{\frac{1}{3}} \Big/ \left\{1 - 2{\cdot}82\left[\zeta + \frac{0{\cdot}5}{\zeta} - \frac{0{\cdot}1}{\zeta^2} - \frac{0{\cdot}8}{\zeta\, Pr}\left(\zeta - \frac{0{\cdot}25}{\zeta} + \frac{0{\cdot}05}{\zeta^2}\right)\right] \times \left(\frac{N}{\chi}\right)^{-\frac{1}{3}}\right\}. \tag{61}$$

For fluids whose Prandtl numbers are below unity, equation (61) is always applicable.

For fluids whose Prandtl numbers are above unity, equation (61) is applicable when $\hat{\omega}/Re$ is large enough to satisfy the above condition. In

Fig. 5, Nu/Nu_0 is shown for $Pr = 0{\cdot}7$ and $\hat{\omega}/Re = 0{\cdot}1$.

In order to estimate the applicable ranges of λ^*/λ_0 and Nu/Nu_0 obtained above, δ and δ_T for $Pr = 0{\cdot}7$ are shown in Fig. 6. The thickness

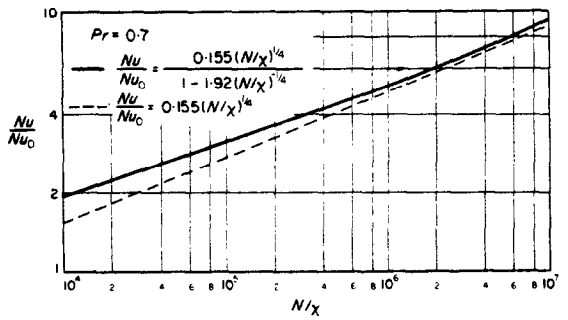

FIG. 5. g_1.

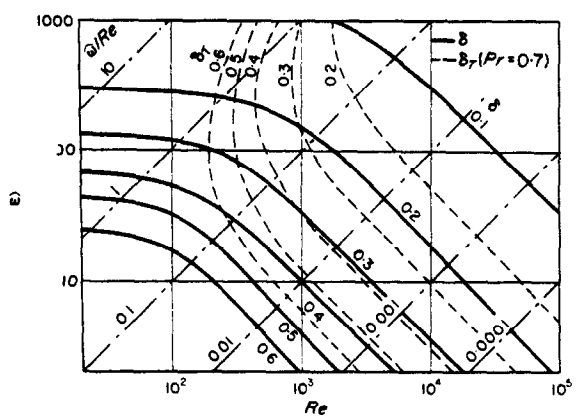

FIG. 6. Nu/Nu_0 vs. (N/χ). $(Pr = 0{\cdot}7,\ \omega/Re = 0{\cdot}1)$.

δ is calculated from equations (30, 32, 35), and δ_T is calculated by putting $Pr = 0{\cdot}7$ in equation (54). Figure 6 shows how δ and δ_T vary with $\hat{\omega}$ and Re. For δ and $\delta_T = 0{\cdot}6$, the correction of δ_2 is close to 10 per cent in the range where Re is large. According to Trefethen's experiment [5] the critical Reynolds number increases as the angular velocity of the pipe increases; to 3900 at $\hat{\omega} = 50$ and 12600 at $\hat{\omega} = 500$. This fact shows the effect of the secondary flow stabilizing the flow and increasing the critical Reynolds number which is observed also in a curved pipe [1] and a heated horizontal pipe [7]. Therefore, the results of analysis for the laminar region are still available when Re is considerably large.

However, in the range where $\hat{\omega}/Re$ is very small, it is necessary to take account of the higher order approximation of δ because of a relatively narrow applicable range bounded by a low critical Reynolds number and a high value of δ as shown in Fig. 6.

The present results can be used up to about $\delta = 0{\cdot}6$ by considering the correction term calculated from equation (35). The maximum error is estimated to be about 5 per cent at the upper limit of δ.

The applicable range of the present analysis is also bounded by $\hat{\omega}/Re < 1/\delta$.

When Nusselt numbers are calculated by equations (60) and (61), it is necessary to bear in mind that the availability of these equations is determined by the value of δ when $\delta_T \leqslant \delta$ and by that of δ_T when $\delta_T \geqslant \delta$.

3.2. *The analysis under the condition of uniform wall temperature*

3.2.1. *Temperature in the flow core.* The same procedure as that used for a curved pipe [6] is applied to the present problem.

Non-dimensional temperature g is defined by

$$g = \frac{T_w - T}{T_w - T_m}. \tag{62}$$

The region under consideration is far from the entrance of the pipe. Hence, T is expressed by using an eigenvalue α_0' as follows:

$$T_w - T \propto \exp(-\alpha_0' Z).$$

Therefore, $T_w - T_m \propto \exp(-\alpha_0' Z)$ and it is found that $\partial g/\partial z = 0$. Putting $\alpha_0' a = \alpha_0$, we have the energy equation in non-dimensional form as

$$\frac{\partial}{\eta\,\partial\eta}(\eta q_\eta) + \frac{\partial q_\psi}{\eta\,\partial\psi} = \alpha_0 w g \tag{63}$$

where q_η, q_ψ are expressed in the same form with those in equation (39). In the core region, we may put $q_\eta = u_1 g_1$, $q_\psi = v_1 g_1$.

From equations (7, 9, 63) the energy equation for the core region is obtained by using the co-ordinate $x = \eta \cos\psi$ as follows:

$$D\frac{dg_1}{dx} = \alpha_0 \left[A + \left(\frac{C}{D} - \hat{\omega}\right)x\right] g_1. \quad (64)$$

The solution of equation (64) is

$$g_1 = \bar{N} \exp\left\{\frac{\alpha_0}{D}\left[Ax + \frac{1}{2}\left(\frac{C}{D} - \hat{\omega}\right)x^2\right]\right\} \quad (65)$$

where $\bar{N}$ is constant.

Since the variation of g_1 in a cross section is supposed to be small, g_1 given by equation (65) is expanded as follows:

$$\begin{aligned} g_1 = \bar{N}\Bigg\{1 &+ \frac{\alpha_0}{D}\left[Ax + \frac{1}{2}\left(\frac{C}{D} - \hat{\omega}\right)x^2\right] \\ &+ \frac{\alpha_0^2}{2D^2}\left[Ax + \frac{1}{2}\left(\frac{C}{D} - \hat{\omega}\right)x^2\right]^2 \\ &+ \frac{\alpha_0^3}{6D^3}\left[Ax + \frac{1}{2}\left(\frac{C}{D} - \hat{\omega}\right)x^2\right]^3 + \ldots\Bigg\} \\ = \bar{N}\Bigg\{1 &+ \frac{\alpha_0 A}{D}x + \frac{\alpha_0}{2D}\left[\left(\frac{C}{D} - \hat{\omega}\right) + \frac{\alpha_0 A^2}{D}\right]x^2 \\ &+ \frac{\alpha_0 A}{D}\left[\frac{\alpha_0}{2D}\left(\frac{C}{D} - \hat{\omega}\right) + \frac{\alpha_0^2 A^2}{6D^2}\right]x^3 + \ldots\Bigg\}. \end{aligned} \quad (66)$$

The constant $\bar{N}$ is determined by the following condition derived from equation (62).

$$\frac{2}{\pi Re}\int_{-\pi}^{\pi}\int_{0}^{1} wg\eta \, d\eta \, d\psi = 1. \quad (67)$$

For g in equation (67), g_1 of equation (66) is substituted. When the initial three terms of the series in the right-hand side of equation (66) are taken into account, $\bar{N}$ is obtained as

$$\bar{N} = \frac{1}{1 + \frac{3}{8}\frac{\alpha_0}{D}\left(\frac{C}{D} - \hat{\omega}\right) + \frac{1}{8}\frac{\alpha_0^2 A^2}{D^2}}. \quad (68)$$

3.2.2. *Temperature in the boundary layer.* Temperature in the boundary layer g is given by equation (43) or (44). But in this case, $g_{1\delta}$ and $g_{1\delta_T}$ are obtained by putting respectively $x = (1 - \delta)\cos\psi$ and $x = (1 - \delta_T)\cos\psi$ in equation (60).

The equation corresponding to equation (46) for the present case is

$$\left(\frac{\partial g}{\partial \xi}\right)_{0m} = \frac{\alpha_0}{4} Re\, Pr \quad (69)$$

Substituting equations (43) and (44) into equation (69) and assuming $\delta, \delta_T \ll 1$, we have

$$\begin{aligned} \left(\frac{\partial g}{\partial \xi}\right)_0 = g_{1\delta}\frac{2}{\zeta\delta} = \frac{2\bar{N}}{\zeta\delta}\Bigg[\Bigg[1 &+ \frac{\alpha_0}{2D}\left[\left(\frac{C}{D} - \hat{\omega}\right) + \frac{\alpha_0 A^2}{D}\right]\cos^2\psi + \frac{\alpha_0 A}{D}\Bigg\{1 + \Bigg[\frac{\alpha_0}{2D} \\ &\times \left(\frac{C}{D} - \hat{\omega}\right) + \frac{\alpha_0^2 A^2}{6D^2}\Bigg]\cos^2\psi\Bigg\}\cos\psi\Bigg]. \end{aligned} \quad (70)$$

From equation (70), the mean value of $(\partial g/\partial\xi)_0$ is obtained as

$$\left(\frac{\partial g}{\partial \xi}\right)_{0m} = \frac{2}{\zeta\delta}\bar{X} \quad (71)$$

where

$$\bar{X} = \frac{1 + \frac{1}{4}\frac{\alpha_0}{D}\left(\frac{C}{D} - \hat{\omega}\right) + \frac{1}{4}\frac{\alpha_0^2 A^2}{D^2}}{1 + \frac{3}{8}\frac{\alpha_0}{D}\left(\frac{C}{D} - \hat{\omega}\right) + \frac{1}{8}\frac{\alpha_0^2 A^2}{D^2}}. \quad (72)$$

Within the range of Re and $\hat{\omega}$ under consideration in the present analysis, we may put $\bar{X} \approx 1$. Hence, from equations (69) and (71) the eigenvalue α_0 is determined as follows:

$$\alpha_0 = \frac{8}{\zeta\delta\, Re\, Pr}. \quad (73)$$

The boundary-layer thickness ratio ζ is obtained from the following energy integral equation of the boundary layer

$$\frac{1}{Pr}\left(\frac{\partial g}{\partial \xi}\right)_0 = g_{1\delta}\frac{\partial}{\partial \psi}\int_0^\delta v\,\mathrm{d}\xi - \frac{\partial}{\partial \psi}\int_0^\delta gv\,\mathrm{d}\xi + \alpha_0\int_0^\delta wg\,\mathrm{d}\xi. \quad (74)$$

The first and second terms in the right-hand side of equation (74) have the order of magnitude $D(\propto N^{\frac{1}{2}}\chi^{\frac{1}{2}})$, while the third has the order of magnitude $\alpha_0 A\delta = 4/\zeta\, Pr$. Therefore, in the region where D is not small, the third term is negligible. Derivation of the relation between ζ, χ and Pr is done in the same way as that shown in the previous section. Following the same procedure of calculation from equations (71–73), and bearing in mind that we may put

$$g_{1\delta} \approx 1 + \frac{\alpha_0 A}{D}\cos\psi. \quad (75)$$

We have the same results as those given by equations (53) and (54).

3.2.3 *Nusselt numbers.* According to the definition of equation (55), the Nusselt number is expressed by using non-dimensional quantities as follows:

$$Nu = \frac{\alpha_0}{2}Re\,Pr = \frac{4}{\zeta\delta} = \frac{0{\cdot}945}{\zeta}\left(\frac{N}{\chi}\right)^{\frac{1}{2}}. \quad (76)$$

Equation (76) is the same as the following equation which is obtained as Nu in the first approximation for the case of a constant wall temperature gradient

$$Nu = \frac{0{\cdot}216}{\zeta}\left(\frac{N}{\chi}\right)^{\frac{1}{2}} \times \frac{48}{11}. \quad (77)$$

Equation (77) is obtained by multiplying Nu_0 to Nu/Nu_0 in equations (60) or (61) and neglecting the correction terms in the denominator.

We may conclude that the Nusselt number is almost independent of the wall temperature, whether it is changing linearly in the axial direction or kept uniform. But the ratio of Nu to Nusselt number for Poiseuille flow in the present case becomes

$$\frac{Nu}{Nu_0} = \frac{0{\cdot}258}{\zeta}\left(\frac{N}{\chi}\right)^{\frac{1}{2}} \quad (78)$$

which is different from that obtained for the case of a constant wall temperature gradient because of the different value of Nu_0, in this case $Nu_0 = 3{\cdot}66$.

4. CONCLUSIONS

In a straight circular pipe rotating around the perpendicular axis, Coriolis force causes a secondary flow perpendicular to the pipe axis.

A fully developed laminar flow field and a temperature field are analysed theoretically, and the following conclusive results are obtained.

(1) It is assumed that a large secondary flow is caused by Coriolis force, and velocity and temperature distributions are distorted considerably from the symmetrical ones in a stationary pipe. By assuming a boundary layer along the wall, the increase in the resistance coefficient due to a secondary flow is obtained. The effect of Coriolis force is remarkable when the value (N/χ) is large. The parameter N is the product of Re and $\hat{\omega}$, where $\hat{\omega}$ is the ratio of Coriolis force to viscous force, and χ, the function of $\hat{\omega}/Re$, represents the effect of Coriolis force in the axial direction caused by the secondary flow. The theoretical result is in agreement with the experimental results obtained in a pipe of sufficiently large length to diameter ratio.

(2) The analysis of the temperature field is done by the same procedure as that for flow field, by assuming a temperature boundary layer along the wall under the condition of a constant wall temperature gradient. The ratio of temperature to velocity boundary-layer thickness

(δ_T/δ) is obtained as the function of Pr and $\hat{\omega}/Re$, and Nusselt number formulae including parameters Pr and $\hat{\omega}/Re$ are obtained to the second order of approximation for relatively large (N/χ).

(3) The analysis done under the condition of a uniform wall temperature shows that the Nusselt number is independent of whether the wall temperature is changing linearly in the axial direction or kept uniform.

REFERENCES

1. Y. MORI and W. NAKAYAMA, Study on forced convective heat transfer in curved pipes (1st report, laminar region), *Int. J. Heat Mass Transfer* **8**, 67–82 (1965).
2. Y. MORI and W. NAKAYAMA, Study on forced convective heat transfer in curved pipes (2nd report, turbulent region), *Int. J. Heat Mass Transfer* **10**, 37–59 (1967).
3. Y. MORI and K. FUTAGAMI, Forced convective heat transfer in uniformly heated horizontal tubes, 2nd report—theoretical study on the effect of buoyancy, *Trans. Japan Soc. Mech. Engrs* **32**(233), 88–97 (1966).
4. Y. MORI and W. NAKAYAMA, Forced convective heat transfer in a straight pipe rotating around a parallel axis (1st report, laminar region), To be published.
5. L. TREFETHEN, Flow in rotating radial ducts, General Electric Co. Report No. 55GL 350-A (1957).
6. Y. MORI and W. NAKAYAMA, Study on forced convective heat transfer in curved pipes (3rd report, theoretical analysis under the condition of uniform wall temperature and practical formulae), *Int. J. Heat Mass Transfer* **10**, 681–695 (1967).
7. Y. MORI, K. FUTAGAMI, S. TOKUDA and M. NAKAMURA, Forced convective heat transfer in uniformly heated horizontal tubes, 1st report—experimental study on the effect of buoyancy, *Int. ... Heat Mass Transfer* **9**, 453–463 (1966).

Résumé— On a analysé théoriquement des champs d'écoulement laminaire et de température entièrement développés dans un tuyau tournant rapidement autour d'un axe perpendiculaire, en supposant l'existence de couches limites dynamique et thermique le long de la paroi du tube. Le coefficient de frottement et le nombre de Nusselt sont obtenus sans la région des grandes valeurs de (N/χ). Le paramètre N est le produit de Re et de $\hat{\omega}$, où $\hat{\omega}$ est le rapport de la force de Coriolis à la force de viscosité et χ représente l'effet de la force de Coriolis provoquée par l'écoulement secondaire. On montre que le coefficient de frottement et le nombre de Nusselt augmentent de façon remarquable, à cause d'un écoulement secondaire produit par la force de Coriolis. On montre aussi en analysant les deux conditions de températures pariétales, c'est-à-dire, le gradient de température pariétale constant et la température pariétale uniforme, que le nombre de Nusselt est presque le même pour ces deux conditions.

Zusammenfassung—Das voll ausgebildete Strömungs- und Temperaturfeld in einem sich schnell um die senkrechte Achse drehenden Rohr wurde theoretisch analysiert; dazu wurden Geschwindigkeits- und Temperaturgrenzschichten entlang der Rohrwand angenommen. Der Widerstandskoeffizient und die Nusselt-Zahl wurden erhalten im Bereich grosser Werte von (N/χ). Der Parameter N stellt das Produkt dar aus Re und $\hat{\omega}$, wobei $\hat{\omega}$ das Verhältnis von Corioliskraft zu Zähigkeitskraft angibt und χ den Einfluss der Corioliskraft auf Grund der Sekundärströmung bedeutet. Es wird gezeigt, dass der Widerstandskoeffizient und die Nusselt-Zahl infolge der von der Corioliskraft bewirkten Sekundärströmung erheblich zunehmen. Die Analyse der beiden Wandtemperaturbedingungen, nämlich konstanter Gradient oder einheitliche Temperatur, ergibt, dass die Nusselt-Zahl für beide dieser Bedingungen nahezu die gleiche ist.

Аннотация—Теоретически изучается полностью развитый ламинарный режим (динамический и тепловой) в трубе, быстро вращающейся вокруг оси. При этом предполагается существование динамического и теплового пограничного слоя. Определены коэффициент сопротивления и число Нуссельта в области больших значений (N/χ). Параметр N есть произведение $Re\hat{\omega}$, где $\hat{\omega}$ — отношение кориолисовой силы к силе вязкости, χ учитывает влияние кориолисовой силы вследствие вторичного потока. Показано, что коэффициент сопротивления и число Нуссельта значительно увеличиваются за счёт вторичного потока, вызванного кориолисовой силой. Показано, что число Нуссельта почти одинаково для двух температурных условий на стенке: постоянный температурный градиент и неизменная температуры стенки.